1st General Report for TC 203
Seismic response of soils, foundations and geotechnical structures

1er rapport général du TC 203
Réponse sismique des sols, des fondations et des ouvrages géotechniques

Semblat J.-F.
Université Paris-Est, IFSTTAR, Dept of Geotechnical Eng., Environment, Natural Hazards and Earth Sciences

ABSTRACT: This session is mainly dedicated to the seismic response and stability of soils, foundations and geotechnical structures. The various following sub-topics are discussed: site effects and soil seismic response (strong seismic motion and seismic hazard in urban areas), landslides (shaking table tests with vertical and horizontal loadings), in situ tests (soil penetrometric characterization, pseudostatic load tests on piles), soil behaviour and liquefaction (Prevost vs Drucker-Prager models, response-envelopes method), earth works stability (retaining walls and excavations, earth dams and embankments), soil improvement (stiff columns, stone columns, soil pillows), seismic isolation techniques (seismic wave screening, isolating foundation system), piles and foundations (performance-based Limit States Design, windmill foundations, Dynamic Hereditary creep theory), numerical modelling (3D FEM simulations for multi-arch culverts, earth pressure coefficients on vertical rigid walls, response of a suspension bridge anchor block to oblique-slip fault movement, dynamic behaviour of a 3D soil-foundation-building system with a seismic isolation). The findings from these papers are synthetized in this report and the links between experimental, theoretical and numerical approaches are discussed.

RÉSUMÉ : Cette session est consacrée à la réponse sismique et la stabilité des sols, des fondations et des ouvrages géotechniques. Les principaux thèmes abordés sont: les effets de site et la réponse sismique des sols (mouvements forts, aléa sismique en milieu urbain), mouvements de terrain (essais sur table vibrante avec chargements sismiques vertical et horizontal), essais in situ (caractérisation des sols au pénétromètre, essais de pieux pseudostatiques), comportement des sols et liquéfaction (modèles de Prevost et Drucker-Prager, méthode des réponses enveloppes), stabilité des ouvrages en terre (soutènements et excavations, barrages et remblais), amélioration des sols (colonnes ballastées, matelas de répartition), isolation sismique (écrans vibratiles, fondation isolante), pieux et fondations (conception en performance, fondations d'éoliennes, théorie du fluage), modélisation numérique (simulations 3D par éléments finis d'ouvrages multi-arches, coefficients de poussée-butée sur murs rigides verticaux, réponse d'un pont suspendu ancré à une mouvement de faille oblique, réponse dynamique 3D d'un système sol-fondation-bâtiment avec isolation sismique). Les résultats des articles sont synthétisés dans ce rapport et la complémentarité entre approches expérimentales, théoriques et numériques est discutée.

KEYWORDS: Site effects, landslides, in-situ tests, soil behaviour, liquefaction, stability, improvement, isolation, piles, modelling.

This session is mainly dedicated to the seismic response of soils, foundations and geotechnical structures. The various subtopics are identified in the following sections as: 1/ Site effects and soil response, 2/ Landslides, 3/ In situ tests, 4/ Soil behaviour/liquefaction, 5/ Earth works stability, 6/ Improvement, 7/ Seismic isolation, 8/ Piles/foundations, 9/ Numerical modelling. 31 papers are reviewed in this report and the link with the various topics is detailed in Table 1. For each paper, this table identifies the main topic by a capital bold **X** and secondary topics by lower case non-bold x.

A general discussion on all the papers and topics is proposed in the last section.

1 SITE EFFECTS AND SOIL RESPONSE

1.1 *Numerical modelling of strong seismic motion*

Paper #2895 by Santisi et al. proposes a numerical approach to model the unidirectional (1D) propagation of a three components (3C) earthquake for seismic response analyses of horizontal multilayer soils. A 3D nonlinear MPII constitutive model is considered. Propagating a 3C signal induces a multiaxial stress interaction decreasing soil strength and increasing nonlinear effects. The nonlinear seismic response of several Tohoku soil profiles are compared in between 1D-3C computations (Fig.1, left) and 1D-1C case (Fig.1, right).

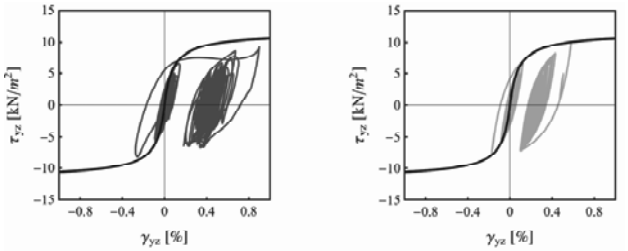

Figure 1. 1D-3C (left) and 1D-1C (right) seismic response for the Tohoku event at site FKS011/FKS015: shear stress/strain loops at 2 m (Santisi et al., #2895).

Paper #3013 by Tabatabaie et al. investigates how stratifications and sub-layers can affect the seismic amplification ratio. Field observations (boring, boreholes) in Bam, Iran show some contradictions between the expected amplifications from EC8 soil types (esp. type E) and the actual amplification levels. To explain such a discrepancy, the authors discuss the effect of sub-layers thickness through a detailed 1D equivalent linear sensitivity analyses (EERA software). These analyses show that the thickness of E, B and D type soil layers and seismic amplification ratios are closely linked. This study reveals the deficiencies of current earthquake codes (e.g. average shear wave velocity) and it emphasizes the effect of sub-layers properties (esp. very soft and very stiff ones) on amplification ratio.

Table 1. Link between the various papers and the different topics: the main topic is identified by a capital bold **X** and secondary topics by a lower case non-bold x.

themes \ papers	site effects	landslides	in situ tests	behav/liquef	earth works	improvemt	isolation	foundations	modelling
1676			x				**X**		
1697				x	**X**				x
1745				x		**X**			x
1759				**X**	x				x
1766					**X**				
1878						**X**			
1886				x		**X**			
2072								**X**	
2080			**X**	x		x			
2153							**X**	x	x
2250		**X**							
2293				**X**				x	x
2299									**X**
2337				x	**X**				x
2360				**X**					
2441								**X**	x
2571				x	**X**	x			x
2628				x	**X**				x
2630								**X**	x
2751					**X**				x
2818			**X**		x				
2846					**X**				x
2895	**X**								x
2918			**X**					x	
2932	**X**								
3013	**X**		x						
3031								**X**	
3052								x	**X**
3064								x	**X**
3065			x	x				**X**	
3086	**X**		x						x

1.2 *Seismic hazard in urban areas*

In paper #3086 by Barchiesi et al., seismic site effects in the urban area of Mendoza (Argentina) are computed from velocity profiles derived from SPT correlation equations. Accounting for the local seismicity, maps of surface amplifications and design spectra are then plotted. As shown if Fig.2, for Zone 2 (shallow sands and silts overlaying gravels with high sehar wave velocity), the computed response spectra are much larger than the design spectrum for such a site. Strong site effects are thus expected in this area and depend on both the velocity contrast and the excitation level.

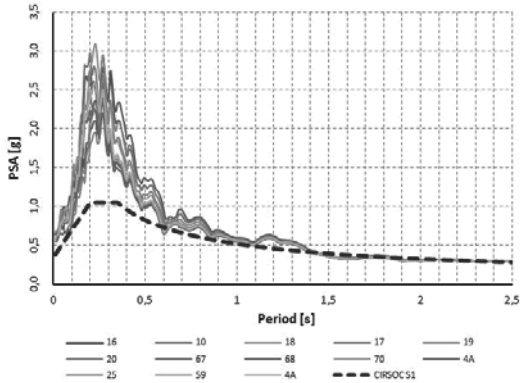

Figure 2: Response spectra in Mendoza (Z2, CIRSOC103, Ao = 0.35g)

Paper #2932 by Kegyes-Brassai et al. deals with a rapid seismic assessment of a large number of buildings using a forecasting approach. The steps involve the determination of the hazard and the computation of building vulnerability (bilinear approximation of the capacity curve). Damages can then be estimated from expected PGAs in a given area.

2 LANDSLIDES

Only one paper (#2250) is dedicated to landslides triggered by earthquakes. In this paper, Shinoda et al. discuss shaking table tests of a large slope model subjected to vertical and horizontal seismic loading. Both sinusoidal and actual seismic excitations are considered. As shown in Fig.3, the results clearly show that a critical direction of the vertical and horizontal accelerations exists, which is a factor to decrease the slope stability. This critical direction of acceleration is generally found to be parallel to the slope inclination.

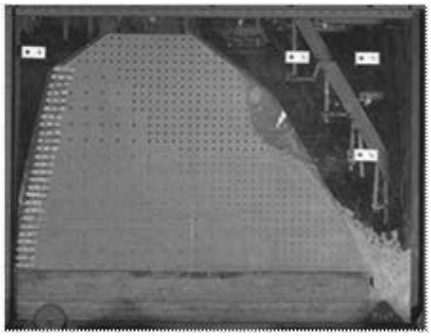

Figure 3. Slope failure under recorded seismic excitation, Shinoda et al.

3 IN SITU TESTS

Two papers are proposed on this topic: one on soil characterization and one on pile tests.

Paper #2818 by Fourie at al. discusses the interest of the PANDA penetrometer to estimate the relative density of soils, which is a useful indication of liquefaction susceptibility. This paper describes an approach for managing upstream TSFs (Tailings storage facilities) using the PANDA for regular in-situ testing (coupled with laboratory compressibility measurements). The PANDA penetrometer is used to characterize the initial state and predict the future state of tailings once buried to a significant depth. The sensitivity to the moisture content requires further researches in order to assess the liquefaction susceptibility in a reliable way.

In paper #2918, Rinaldi et al. present pseudostatic load tests to evaluate the bearing capacity of large diameter piles. The performed tests show that using moderate loads (10 to 20 tons falling from 10 cm to 120 cm) allows to reach more than 800 tons of loading and the full mobilization of the pile ultimate capacity. The distribution of reaction forces along the pile shaft is shown in Figure 4.

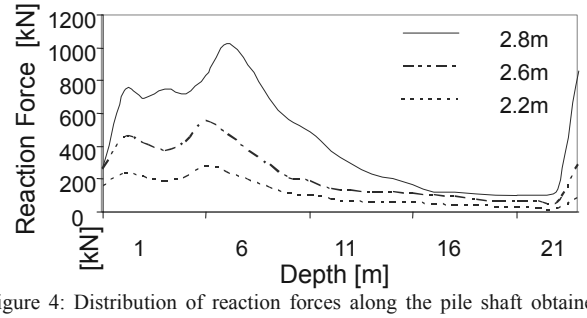

Figure 4: Distribution of reaction forces along the pile shaft obtained from the solution of the wave equation for different drop height of the mass (Rinaldi et al, #2918).

It seems that most of the load is taken by the shaft and only 900 kN are taken by the tip at the maximum load of the test performed. The behaviour of pile-soil systems corresponds to a quasi elastic phase with little plastic deformations. The main advantages of the proposed pseudostatic tests is the possibility to apply load increments.

4 SOIL BEHAVIOUR/LIQUEFACTION

The possibilities of the Prevost's model are highlighted by Cerfontaine et al. (paper #1759) and compared to that of a classical Drucker-Prager model. The Prevost's model is able to capture the main features of the cyclic behaviour of soils, namely popre pressure build-up and plastic deformation accumulation. As an illustration, a suction caisson, part of a tripod offshore foundation for wind turbines is modelled. As shown in Fig.5, the difference between both models is limited during the first part of the loading. Conversely, during the second part, the soil characterized by Prevost's model shows a continuous decrease of mean effective stress without reaching a stationary state. The results computed through this model also show pore pressure and plastic deformation accumulation which the Drucker-Prager model is unable to represent.

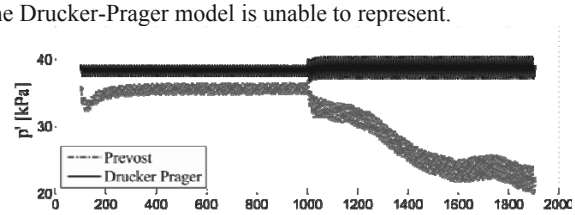

Figure 5: Comparison between mean effective stresses at 0.5m depth under the top of the suction caisson for Prevost and Drücker-Prager models (Cerfontaine et al, #1759).

To assess the soil behaviour, the experimental method of response-envelopes is discussed in paper #2360 (Hettler et al.). The stress-path-dependent strain behaviour at low-cycle loading is studied through drained, stress-controlled triaxial-tests. The cyclic load in the first direction is repeated until the measured strains are practically reversible or rather quasi-elastic. It is found that quasi-elastic behaviour can already occur at low numbers of cycles. The strain response of the last cycle is evaluated and plotted. After that, the test is continued with the same stress increment, but in a different direction in the stress-space until quasi-elastic behaviour occurs again. In the response-envelopes (Fig.6), it is found that the size of the ellipses decreases with increasing mean pressure p and the ellipses rotates depending on the initial stress state (stress-induced anisotropy).

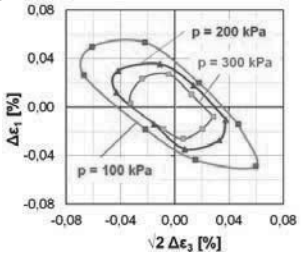

Figure 6: Comparison of response-envelopes due to $\Delta\sigma = 50$ kN/m² for 3 different mean pressures p and constant initial stress-ratio $\eta = 0{,}75$ (Hettler et al, #2360).

In paper #2293, Nakai et al. investigates the seismic stability of a steel fabricated column constructed on liquefiable grounds with various stratigraphies. A dynamic/static soil-water coupled finite deformation analysis is performed in the framework of the Finite Element Method. From the results, it is found that the plastic deformation is predominant in the liquefied sand layer, which led to a decrease in acceleration at the ground surface. However, if the embedment depth was shallow with high gravity center, the structure would still incline easily due to the loss of bearing capacity by liquefaction in the subsurface layer and gradually tilt under its own weight.

When there is a clay layer seated on the liquefiable layer, the accelerations are amplified in the clay layer leading to an increase of input acceleration for the liquefiable layer, and there is thus a risk that the oscillations of the structure would be increased. In particular, when the thickness of the liquefiable layer is small, the attenuation of the acceleration in the liquefiable layer is also small, so the stability of the structure above is significantly reduced.

5 EARTH WORKS STABILITY

5.1 *Retaining walls and excavations*

A simplified method is proposed by Serratrice (paper #1697) to find the equilibrium of a wall submitted to seismically induced pseudo-static loads. The failure mechanism involves two wedges. The example of a purely frictional soil is depicted in Fig.7. The angle between the horizontal axis and the direction of the pseudo-static force is denoted α. The computation is performed in three iterations on the friction angle to reach equilibrium (for $\phi = 29.5$). The value of α is approximately $\alpha = 210$. As shown in Fig.7, the moduli S of the forces do not correspond to the maximum of the active force and the minimum of the passive force. The results compare well with that from Shukla et al. (2009).

The method is also extended with the introduction of water pressures. The equilibrium is then considered in terms of effective stresses. It allows the comparison between both cases (effective stresses and total stresses).

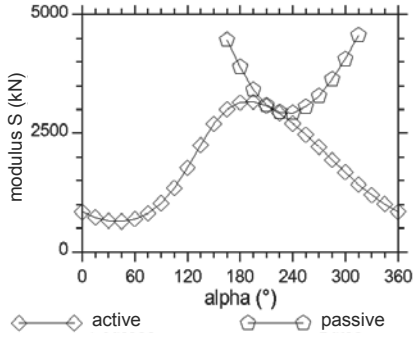

Figure 7: Active and passive earth pressures with respect to angle α for a soil resistance leading to the equilibrium of a wall (Serratrice, #1697).

In paper #2628 by Khomyakov, the excavation of deep ditches is investigated in order to determine the optimum scheme of excavation and slope fixing strategy. Laboratory experiments in a tray show the efficiency of soil anchors to ensure the stability of the slope of a ditch. Numerical simulations are also performed for an optimal design of the anchoring system (number of lines, length, etc). The optimal parameters depend on the soil type.

5.2 *Earth dams, embankments*

Four papers deal with the seismic response and stability of earth dams and embankments.

The safety conditions of embankments in static and seismic conditions are investigated by Gottardi et al. (1766) as a function of the soil parameters variability, seismic hazard features and considering various relevant river water levels. Geotechnical and geological field investigations are conducted in order to identify several representative sections of the riverbank. Detailed field and laboratory soil characterizations are then performed (CPTU, oedometric, resonant column). From these parameters, static and seismic stability analyses are proposed. Stability maps of the investigated area based on the data spatial variability are derived (probabilistic approach).

Paper #2337 (Shimizu and Yamada) discusses the effect of seismic waves on the delayed failure behaviour of earth works. The natural frequencies and natural modes of the whole soil structure-ground system are calculated first. The embankment is then assumed to be saturated and elasto-plastic finite elements represent the two-phase soil-water media to simulate the whole consolidation process. For the constitutive equation for the soil skeleton, the elasto-plastic constitutive equation "SYS Cam-clay model" is considered for the ground and an embankment constructed on it (soil-water 2-phase system). Seismic response analyses, in frequency bands close to the natural frequencies of the structure-ground system, are carried out. Various delayed failure behaviours are found: they may develop from the ground to the embankment (case 1, Fig.8) or from the embankment to the ground.

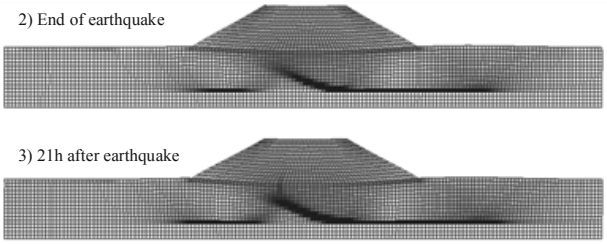

Figure 8: Slip surface (case 1) developing from ground to embankment (Shimizu, 2337).

The structural stability of an earth dam is also investigated by Srivastava and Babu (paper #2571). In this work, a geosynthetics lining system is used as a seepage barrier. The static and dynamic stability of the dam is studied numerically. A dynamic numerical analysis is also performed considering a sinusoidal excitation as well as Bhuj earthquake recordings. The results clearly show that geosynthetics lining system enhance the stability of the dam sections. In the static case, the factor of safety is increased 1.45 times. In the dynamic case, the maximum displacement at the dam crest is only one third of that of the case where there is no geosynthetics. It is due to the strong reduction of the excess pope water pressure.

In paper #2751, Athanasopoulos-Zekkos and Seed perform dynamic 2D equivalent linear, finite element numerical analyses to obtain accelerations and shear stresses for three levee profiles in California. Four sliding surfaces are pre-selected based on previous slope stability analyses for identifying the most critical sliding surfaces, and the seismically induced deviatoric displacements are computed using a Newmark-type approach. As suggested by Seed and Martin (1966), the effects of the dynamic response of the sliding mass itself can be significant in the overall displacements. Therefore, the concept of the equivalent acceleration time history is used to account for this effect. 1,500 ground motions (from the Pacific Earthquake Engineering Research Center, NGA strong motion database) are used to develop statistically stable estimates of dynamic response of the levees and to provide insight towards the effect of ground motion selection to the dynamic response of earthen levees. Four groups of input ground motions were used in the analyses, each group scaled to a specified PGA_{input}: 0.1g, 0.2, 0.3g, and 0.4g respectively.The magnitude of the seismically induced displacements depend on the seismic resistance of the earth embankment (k_y) and the seismic demand (k_{max}). Figure 9 shows the calculated displacements increase for a given k_y/k_{max} ratio and for PGA_{input}=0.2g. They are between the two bounds proposed by Makdisi and Seed (1978), but still closer to the lower bound curve. This provides an important insight as to how to interpret these bounds for different shaking intensities, within the same magnitude bin. From these results, recommendations are made on evaluating seismically-induced deviatoric displacements for levees.

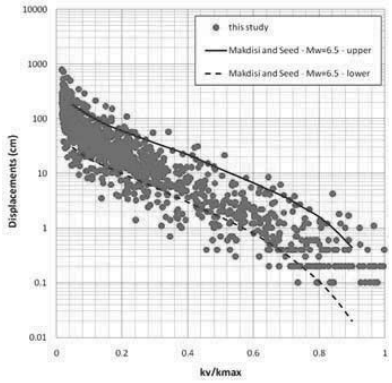

Figure 9. Seismic displacements for motions with M_w=6.5 to 7.0 and PGA_{input}=0.2g, for Levee A (Athanasopoulos-Zekkos and Seed, #2751).

6 IMPROVEMENT

Four papers are dedicated to soil improvement to reduce liquefaction.

Zerfa (paper #1745) models the behaviour of reinforced ground by the finite element method in 2D considering a Bowen mixture formulation. Prevost's model is used for the soil behaviour (saturated porous medium) and the stiff columns embedded in the soil are considered as elastic. Lysmer type absorbing boundaries are implemented. The dynamic simulations involve a Pacoima type accelerogram (PGA limited to 0.25g). As displayed in Fig.10, the pore pressure build up is significantly faster in the unreinforced soil. However, the numerical results show that a large replacement area is mandatory to mitigate liquefaction, reduce pore pressures and settlements between columns.

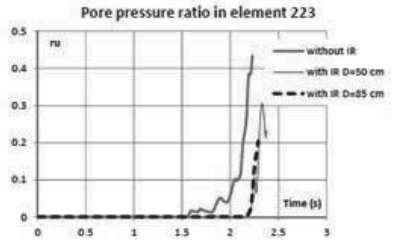

Figure 10. Pore pressure ratio with and without stiff columns (Zerfa, #1745).

In paper #1878, Lambert investigates the response of Mixed Module Columns (CMM®s) to different static and dynamic loads through in situ and laboratory tests (shallow foundation with a group of Mixed Columns). The field tests indicate that the bearing capacity is three time larger than that of the original soil and the settlements are found to be 4 to 5 times less. A reduced scale model is also studied through 1g laboratory experiments. The influence of the thickness of the soft part of the Mixed Column of the forces recorded in the stiff part is displayed in Fig.11 as the lateral pressure of the soil p with respect to the lateral displacement of the head of the rigid part, denoted y.

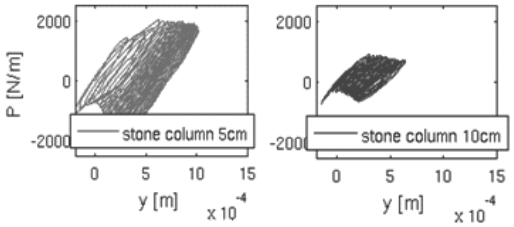

Figure 11. p-y curves at the rigid part head for 5 and 10 cm gravel column (Lambert, #1878).

We can notice that the displacement is much smaller with a column height of 10 cm (maximum displacement: 0.6 mm) that with a 5 cm height (maximum displacement: 1.0 mm). Consequently, thick soft columns must be chosen in order to reduce the forces in the rigid part. Finally, the results indicate that the footing bearing capacity with CMM increases and a large amount of the seismic energy is dissipated within the soil column.

Lambert also discusses the interest and implementation of stone columns (paper #1886). The three main effects are: increase of the Cyclic Resistant Ratio due to the higher soil compacity, reduction of the Cyclic Stress Ratio due to the stress concentration in the stone column and fast decay of the pore pressure due to the high permeability of the gravel. The results depend on the geotechnical conditions at the site: for silt, it is possible to reduce the potential risk of liquefaction by primarily considering the drainage and the effect of stress concentration, whereas for sand the predominant action is compaction. The design of stone columns is also discussed at the end of the paper.

In paper #2080, Usmanov shows that the water saturation of the soil contributes to the transition into the category of weak and high compressibility. To improve the bearing capacity and reduce the compressibility of soils, high-condensed soil pillows are studied. Their efficiency is shown to be very good but their thickness should not be less than 0.75 width of the foundation. Usmanov also investigates vertical sandy drains to improve the behaviour of weak water-saturated loess. These results allow to improve the design and construction of buildings and structures in seismically active areas involving such soils.

7 SEISMIC ISOLATION

Two papers are proposed in the field of seismic isolation: one on seismic wave screening (#1676) and one on seismic isolation at the foundation system (#2153).

In paper #1676, Brûlé et al. proposes field experiments to assess the efficiency of a wave screening system. The test site is located is the Grenoble area in homogeneous thick clayey soils (the layer depth has been estimated around 200m). As shown in Fig.12, the system consists in modifying the global properties of the soil by using a grid of vertical, cylindrical and empty boreholes (spacing 1.73m). They are 5m deep and their diameter is 320mm. The excitation is generated around 50Hz by a vibroprobe and velocimeters are displayed along the free surface (Fig. 12). The surface wave velocity at the site is found to be 78 m/s leading to a wavelength of 1.56m near the source. The experimental results lead to a very strong energy abatment between the second and third rows. The efficiency of the screening system is thus very good and the perspective is now to investigate lower frequency ranges.

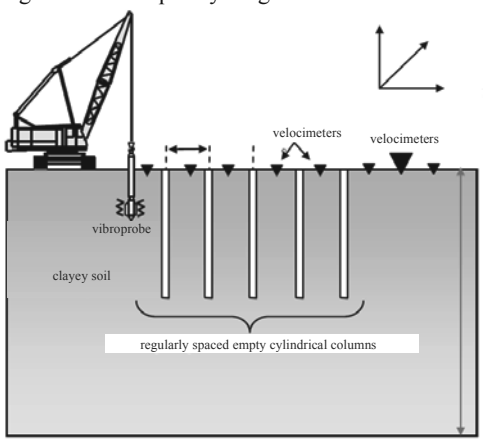

Figure 12. Principle of the wave screening system and experimental set-up (Brûlé et al., #1676).

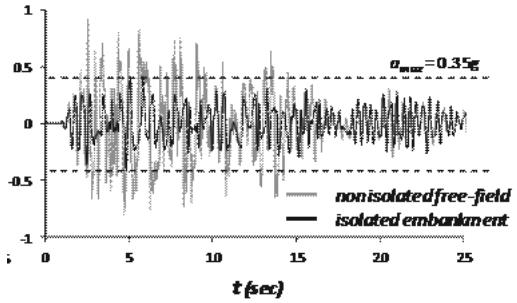

Figure 13. Standard pier response (acceleration) vs pier response with application of the in-soil isolation system (Tsatsis et al., #2153).

A different isolation method is proposed by Tsatsis et al. (paper #2153): a sliding surface comprising two synthetic liner layers is introduced within the foundation soil. The contact between both layers generates some friction and dissipates a significant energy amount. To assess the efficiency of the method, a soil-embankment-pier system is studied numerically.

The geometry of the isolation system is trapezoidal, with isolated wedges on the two sides. The synthetic liners are placed at a depth H = 2 m under the surface. The isolated embankment comprises a dense gravel layer (modelled with a nonlinear constitutive model). The two wedges are filled with pumice, a lightweight material of relatively small stiffness (E = 10 MPa) in order to impose the minimum possible resistance to the sliding motion of the embankment. The superstructure, an idealized bridge pier (for simplicity), is placed on top of the isolated embankment. As shown in Fig.13, the proposed system serves as a fuse mechanism within the soil and substantially reduces the acceleration transmitted onto the structure.

8 PILES/FOUNDATIONS

Five papers are dedicated to foundations and SSI. They mainly concern pile foundations.

Gudavalli et al. investigate 1,355 open-ended piles in dense to very dense sandy soils (paper #2072). These piles are driven down to 10 m and 30 m. The PLR (plug length ratio) values increase with the pile diameter: from 0.76 for 406mm-diameter piles to 0.91 for 914mm-diameter piles. The authors propose an equation giving the PLR as a function of the pile inner diameter. The unit skin friction and unit end bearing values are estimated by performing dynamic load tests (PDA) and signal matching analyses (CAPWAP) on 99 piles. These parameters are found to increase with decreasing PLR. New equations to estimate the skin friction factor β and end bearing factor N_q from the PLR are thus proposed for dense to very dense sands.

Yang presents a performance-based Limit States Design (LSD) approach involving detailed soil-foundation-structure interaction analyses for the Golden Ears Bridge in Vancouver, Canada (paper #2441). Soil-foundation-structure interaction analyses involve both global bridge structural seismic modelling and foundation substructure modelling such as:

- The nonlinear load-displacement response of foundation-soil systems is modelled by hybrid pile group techniques leading to the results displayed in Fig.14.
- The radiation damping of foundation-soil systems is modelled in the form of viscous damping (Novak, 1974).
- The bridge and foundation seismic response are modelled by dynamic time domain FEM computations (Adina) and hybrid foundation models under pseudo-static seismic loads. The results from full scale Osterberg-Cell tests are incorporated in the models.
- The results from full scale tests (Osterberg-Cell and pile load tests) are analyzed in the framework of the performance-based foundation design.

The results of the nonlinear time history FEM analyses show that important soil-structure interaction effects reduce the

foundation seismic forces by about 14% while the foundation seismic displacements increased. Furthermore, the performance-based soil-foundation-structure interaction analyses demonstrate that the pile length can be shortened if increased displacements and rotations of the foundation can be tolerated under the bridge seismic and non-seismic performance criteria.

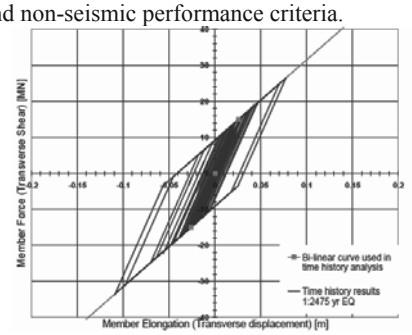

Figure 14. Transverse shear-displacement time history results for Pier M5 using nonlinear inelastic soil springs (Yang, #2441).

In paper #2630, Chang assesses an existing pile foundation through numerical models. He also suggests a new design by checking up the maximum moment of the pile with the moment capacities for the seismicity of interest. The pile displacements correspondent to the moment capacities can be found and used as the allowable pile displacements.

The work of Vintila et al. (paper #3031) investigates the influence of seismic loads in foundation design for aeolian units. It proposes optimal design and construction techniques for different types of foundations on various soil profiles. The parameters are determined in the field from geoeletric studies and in the lab from oedometric as well as trixial tests. The behaviour of shallow foundations may be improved by making a skirt along the foundation edge. The foundation is thus embedded in a rock of good quality and the active surface is increases from 54% up to 70%. Large diameter piles connected to a slab may also be used; it acts as a compensating box and reduces the deformations. Finally, for thick loess layers (20m or more), floating pile foundation may be chosen.

The effect of the loading history on soil-structure systems is analysed by Taranov et al. with respect to the rheological properties of the materials (paper #3065). They treat the integral equations of the creep theory in an algebraic way considering three different sequential processes: linear creeping of the foundation, nonlinear creeping of the base soil and simultaneous creeping of the soil and foundation. By using the Dynamic Hereditary creep theory, they can estimate the foundations settlements (logarithmical increase) due to machinery dynamic loads. As displayed in Fig.15, data obtained from special vibrostamp experimental tests allows to validate the theoretical approach in order to describe the deformation progress with time on steady-state phase of creep.

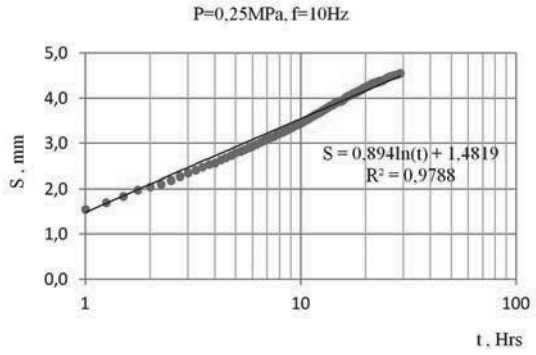

Figure 15. The curve of settlement progress with time a_z=10μm (Taranov et al., #3065).

9 NUMERICAL MODELLING

Four papers are mainly dedicated to numerical simulations even though several other papers involve numerical modelling. In this section, 3D FEM models are always considered.

Dynamic FEM analysis is carried out by Sawamura et al. (#2299) to investigate the influence of spacing between multi-arch culverts and its mechanical behaviour under seismic conditions. In a previous study, dynamic centrifuge tests have been carried out to confirm the difference of dynamic behaviour due to the influence of spacing. Light fill material can be used for the reduction of earth pressure during earthquakes. In the present paper, 3D elasto-plastic FEM simulations are performed for static as well as dynamic loads. For wide unit intervals, large maximum bending moments are found. Figure 16 shows the earth pressure distribution on the boundary portions of the ground and arch culvert when maximum bending moment is generated at right foot. When the arch culvert bends to the left, as a result of seismic force, it turns out that a large earth pressure acts on the right-hand side of arch culvert. Comparing various spacings (from L=0.25H in red to L=1.5H in yellow), the earth pressure becomes higher for larger unit intervals. This could be due to the difference of horizontal displacements of the soil around arch culvert as shown in Figure 16. On the other hand, near the top part of the arch culvert, all cases lead to very close results.

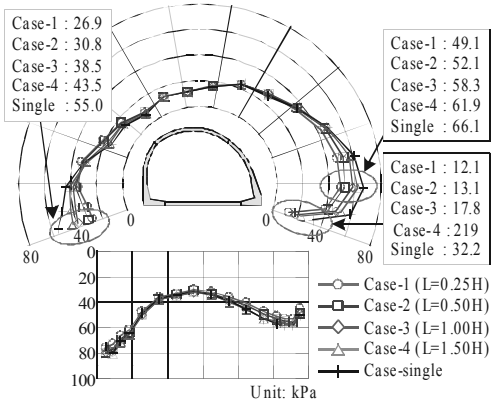

Figure 16. Earth pressure distribution on the boundary portions of the ground and arch culvert when maximum bending moment is generated at right foot (Sawamura et al., #2299).

Since static and seismic earth pressures are often determined from plan strain approaches, a 3D limit analysis numerical approach is proposed by Santana et al. (#2846) to determine seismic active horizontal earth pressure coefficients for vertical rigid walls. In this work, an associated flow rule and perfectly plastic behaviour are assumed. Various aspect ratios (b/h) are considered for the wall and different friction angles for the soil as well as soil-wall interface friction ratios. The applied loads involve the soil weight and equivalent static forces directed towards the wall, equal to $\alpha\gamma$, where α is the seismic horizontal coefficient (α=0, 0.1, 0.2, 0.3, 0.4 and 0.5). No vertical seismic coefficient was considered.

As depicted in Fig.17, the mechanisms involved in the mobilization of the active earth pressures are inferred from the plastic deformation zones. The numerical results show a significant three-dimensional effect of the b/h ratio: for small values of this ratio, there is a significant decrease in the soil seismic horizontal active earth pressure coefficients. For large aspect ratios, the pressure coefficients are very close to the two-dimensional case. The ratios between the 3D and 2D seismic horizontal earth pressure coefficients are found to be independent on the soil/wall friction ratio.

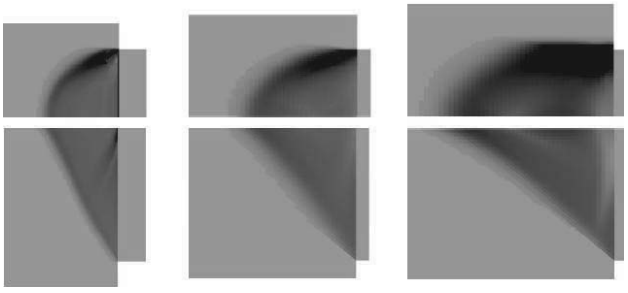

Figure 17. Plastic deformation zones for a friction angle ϕ'=30º, a soil-wall interface friction ratio δ/ϕ'=2/3, and three values of the seismic coefficient α – 0, 0.2 and 0.4 (Santana et al., #2846).

The 3D response of a suspension bridge anchor block to oblique-slip fault movement is modelled by Avar et al. (#3052) using the FEM. The bridge project is located in Izmit Bay (Turkey) where secondary fault systems were evidenced. The lateral and vertical fault displacements are applied at the base of the soil medium (100m deep). The constitutive model adopted is the elasto-plastic model with standard Mohr-Coulomb (MC) yield surface formulation. As the fault propagation through saturated fine-grained soil deposits occurs too fast for excess pore water pressures to dissipate, the analysis has been performed using effective parameters for strength and stiffness in the clay layers. The fault displacements result in the rotation and translation of the anchor block. Figure 18 compares the u_x displacement at the ground surface for the free field and the anchor block-soil models along a line in the x-direction passing through the centre of the soil-anchor block. The difference between free-field and the anchor block-soil model displacements at the anchor block boundaries are significant. The discontinuity in vertical downward movement in the vicinity of the right hand side (footwall side) of the block implies separation between the soil and the block developing. The anchor block also moves 250 mm in the x-direction following the movement of the hanging wall (Fig. 18). The rigid movement of the anchor block is clearly observed in Fig. 18. It is evident that the rigid anchor block introduces a kinematic constraint to the propagating fault. The ground moves slightly towards positive x-direction in the footwall side in the free-field model as seen in Fig. 18 whereas this does not occur when the anchor block is placed.

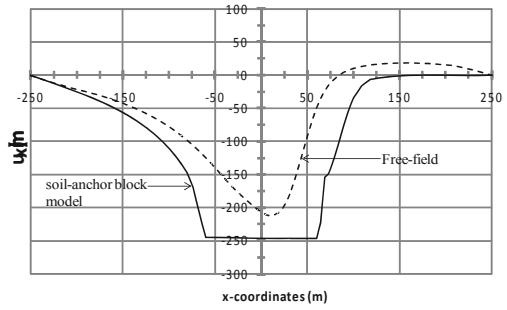

Figure 18. Horizontal displacements, u_x, in the x-direction along the centre of the model at the ground level (Avar et al., #3052).

The dynamic behaviour of a 3D "soil-foundation-building" system with a seismic isolation is investigated by Boykov et al. (#3064). The structure is a real multi-story building, located on a landslide slope in the seismically-active area of the Crimean Republic. The soil base is represented by a talus layer about 10-18 m deep with a shifted mudstone layer (about 3-5 m deep) and an argilite foundation below that. The initial building design called for drilling piles (ϕ=620mm, L=35mm), embedded into the argilite bedrock. The 3D FEM model involve absorbing boundaries and 3C synthetic accelerograms are considered. A non-associative law (modified Mises-Schleicher-Botkin's criterion) is chosen for the soil. Rayleigh damping is also included in the model.

The specification of the work of soil and damper lead to an increase of shifts in the plane of the building. Maximum amplitude increases from 8 to 10 cm. At the maximum amplitude, the shifts are mainly oriented along the action of the radial component of the seismic load. The oscillations in the horizontal plane are thus close to the neutral situation. That is why the building does not have tendencies to horizontal shifts. The consideration of the plastic work of the damping layer allows the calculation of the amplitude decreasing of the oscillations of the top floors of the building. As displayed in Fig. 19, the maximum values of these shifts significantly depend on the constitutive law and they approximately reach 64 cm in the period of time from 15.1 to 24.5 seconds. The process of irreversible building settlement develops to 20 s of load, after which the settlement becomes stable and exceeds at least the value of 13 cm. Finally, due to inertial forces in the soil, areas of significant tensile forces may appear in the piles. These zones are located below the pile heads and must be taken into account when designing grillage for the structure. This work also shows that the utilization of piles during seismic loads in layered soils with various deformation properties leads to the appearance of forces within these piles that can exceed the forces at the pile heads by as much as a factor of two.

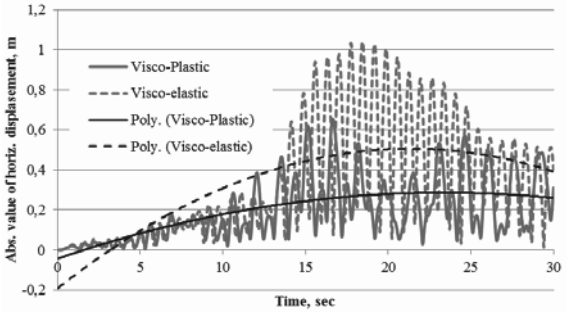

Figure 19. The diagram of absolute value of displacements for upper foundation slab (visco-elastoplastic model) and grillage slab (visco-elastic model), Boykov et al. #3064.

10 DISCUSSION AND CONCLUSION

This session is mainly dedicated to the seismic response and stability of soils, foundations and geotechnical structures. The various sub-topics lead to the main following results:

- *Site effects and soil seismic response*: 1D-3 components simulations allow the analysis of strong seismic motion for the Tohoku quake; for the site of Bam (Iran), some discrepancy is found between the expected amplifications (from EC8 soil types) and actual amplifications; very soft sites may strongly amplify the seismic motion in urban areas.
- *Landslides*: through shaking table tests, a critical direction of the seismic loadings is evidenced.
- *In situ tests*: penetrometric tests characterize the relative density of soils (but difficult for moisture content); pseudostatic tests on piles allow load increments.
- *Soil behaviour and liquefaction* : Prevost's model simulates well pore pressure and plastic strain accumulation; response-envelopes method assesses to sensitivity to mean pressure and stress induced anisotropy.
- *Earth works stability* : yield design allows the analysis of the stability of retaining walls even if water pressures are included; exces spore water pressure may be reduced by geosynthetics; probabilistic approaches assess the influence of the spatial variability of soil parameters on stability; recommandations are made on evaluating seismically induced deviatoric displacements for earthen levees.
- *Soil improvement* : using stiff columns, a large replacement area is mandatory to mitigate liquefaction; depending on the

soil type, stone columns allow to reduce the risk of liquefaction by drainage, stress concentration or compaction; high-condensed soil pillows improve the bearing capacity and reduce the compressibility of soils.

- *Seismic isolation techniques*: a screening system for vibrations/seismic waves is proposed; synthetic liners are proposed to isolate an embankment having a bridge pier on top (sliding motion is thus allowed).
- *Piles and foundations* : for open-ended piles, new equations are proposed to estimate the skin friction and end bearing factor from the plug length ratio; performance-based Limit States Design including soil-foundation-structure interaction allows to reduce the foundation seismic and the pile length; the design of windmill foundations may be optimized accounting for the soil type (e.g. skirt around shallow foundations, floating piles in loess); the effect of the loading history on soil-structure systems is assessed by the Dynamic Hereditary creep theory and vibrostamp experiments.
- *Numerical modelling*: 3D FEM simulations are performed to assess the influence of spacing in multi-arch culverts; earth pressure coefficients on vertical rigid walls are computed by a 3D limit analysis approach for various aspect ratios and compared to 2D values; the 3D response of a suspension bridge anchor block to oblique-slip fault movement is modelled by the FEM, it evidences a kinematic constraint to the propagating fault; the dynamic behaviour of a 3D soil-foundation-building system is studied by the FEM, the forces along the piles may significantly exceed that at the pile heads in layered soils.

11 LIST OF PAPERS

1676: S. Brûlé, E. Javelaud, S. Guenneau, S. Enoch, Vers les métamatériaux sismiques (Towards seismic metamaterials).
1697: J.F. Serratrice, Méthode simplifiée de calcul d'une paroi sous séisme (Simplified seismic wall stability analysis).
1745: F.Z. Zerfa, Analyse sismique couplée des sols renforcés par inclusions rigides (Coupled dynamic analysis of soils reinforced with stiff columns).
1759: B. Cerfontaine, R. Charlier, F. Collin., Possibilities and limitations of the Prevost model for the modelling of cohesionless soil cyclic behavior.
1766: G. Gottardi, C. Madiai, M. Marchi, L. Tonni, G. Vannucchi, Methodological approach for the stability analysis of the Po river banks.
1878: S. Lambert, Colonne à Module Mixte sous des sollicitations statiques et dynamiques : étude expérimentale (Mixed Module Columns under static and dynamic load. Experimental study).
1886: S. Lambert, Evaluation de la réduction du risque de liquéfaction par des colonnes ballastées (Evaluation of liquefaction mitigation by stone columns).
2072: S.R. Gudavalli, O. Safaqah, H. Seo, Effect of soil plugging on axial capacity of open-ended pipe piles in sands.
2080: R. Usmanov, The device of the bases and foundation in the conditions of weak soil and high seismicity activity of the Republic of Tajikistan.
2153: A.K. Tsatsis, I.C. Anastasopoulos, F.L. Gelagoti, R.S. Kourkoulis., Effectiveness of In-soil Seismic Isolation taking account of Soil-Structure Interaction.
2250: M. Shinoda, S. Nakajima, H. Nakamura, T. Kawai, S. Nakamura, Shaking table test of large-scaled slope model subjected to horizontal and vertical seismic loading using E-Defense.
2293: K. Nakai, B. Xu, T. Takaine, Seismic stability assessment of a steel plate fabricated column constructed on liquefiable grounds with different soil-layer profiles.
2299: Y. Sawamura, K. Kishida, M. Kimura, Dynamic behavior of multi-arch culverts embankment considering the installation interval of consecutive arch culverts.
2337: R. Shimizu, S. Yamada, Effect of Seismic Waves with Different Dominant Frequencies on the Delayed Failure Behavior of a Soil Structure-Ground System.
2360: A. Hettler, St. Danne, Strain Response Envelopes for low cycle loading processes.
2441: D. Yang, Performance-based foundation design for seismically induced forces and displacements of major cable-stayed bridges.
2571: A. Srivastava, G. L. Sivakumar Babu, Stability analysis of earth dams under static and earthquake loadings using geosynthetics as a seepage barrier.
2628: V.A. Khomyakov, Ensuring stability of boards of deep ditches in seismic regions.
2630: D.W. Chang, S.H. Sung, S.M. Lee, A. Zhussupbekov, E. Saparbek., On Seismic Performance and Load Capacities for Pile Design.
2751: A. Athanasopoulos-Zekkos, R.B. Seed, Seismic Slope Stability of Earthen Levees.
2818: A.B. Fourie, J H Palma, G Villavicencio and R Espinace, Risk minimisation in construction of upstream tailings storage facilities based on in-situ testing.
2846: T. Santana, N.M.C. Guerra, A.N. Antão, M.Vicente da Silva, Three-dimensional seismic active earth pressure coefficients using upper bound numerical limit analysis: a few preliminary results.
2895: M.P. Santisi L. Lenti, J.F. Semblat, Modélisation 1D-3Composantes de la réponse sismique d'une colonne de sol multicouche à comportement non linéaire (1D-3Component seismic response modelling of a multilayer nonlinear soil profile).
2918: V.A. Rinaldi, R. Viguera, Pseudo-static Pile Load Test: Experience on Pre-bored and Large Diameter Piles.
2932: O. Kegyes-Brassai, R.P. Ray, Applying Two Earthquake Risk Analysis Methods to A Town In Hungary.
3013: S.H. Tabatabaie, M. Hassanlourad, M. Yazdanparast, A. Mohammadi, Evaluation of effective parameters on soil layers seismic amplification ratios (A case study of Bam earthquake).
3031: D. Vintila, D. Tenea, A. Chirica, Foundation conditions analysis for some eolian power units corresponding to the seismic loads influence.
3052: B.B. Avar, A.H. Augustesen, T. Kasper, J.S. Steenfelt, 3D numerical analysis of a suspension bridge anchor block to oblique-slip fault movement.
3064: I.P. Boyko, O.S. Sakharov, V.O. Sakharov, Behavior of a multi-story building under seismic loads when taking into account the viscoplasticity of the soil base.
3065: V.G. Taranov, V.A. Aleksandrovych, I.Ia. Luchkovskyi, S.A. Plashchev, N.V. Kornienko, Structure-soil massif system behavior features via static & dynamic loads.
3086: A.M. Barchiesi, C. Mancipe-Herrera, Seismic site effects in the city of Mendoza and surroundings (Argentina).

12 REFERENCES

Athanasopoulos-Zekkos, A., and Saadi, M. 2012. Ground Motion Selection for Liquefaction Analysis of Earthen Levees, *Earthquake Spectra*, EERI (in press).

Anastasopoulos I., Gazetas G., Loli M., Apostolou M., Gerolymos N. 2010. Soil Failure can be used for Earthquake Protection of Structures, *Bulletin of Earthquake Eng.*, Vol. 8, pp. 309–326.

Asaoka et al. 2002. An elasto-plastic description of two distinct volume change mechanisms of soils. *Soils & Foundations*, 42 (5), 47-57.

Chang, D.W., Yang, T.Y. and Yang, C.L. 2010. Seismic Performance of Piles from PBEE and EQWEAP Analyses, *J. of Geotechnical Engineering*, SEAGS/AGSSEA, Vol. 41, No.2, pp. 79-86.

Hoque, E., and Tatsuoka, F. 1998. Anisotropy in elastic deformation of granular materials. *Soils and Foundations* 38 (1), 163-179.

Paik, K. and Salgado, R., 2003. Determination of bearing capacity of open-ended piles in sand. *Journal of Geotechnical and Geoenvironmental Engineering*, 129(1), pp. 46 – 57.

Prévost J. H., 1978. Plasticity theory for soils stress-strain behavior. *Journal of Eng. Mechanics Division,* 104, EM5, 1177-1194.

Robertson P.K. 2009. Interpretation of cone penetration tests – a unified approach. *Can. Geotechnical J.* 46 (11), 1337 – 1355.

Semblat J.F. and Pecker A. 2009. *Waves and vibrations in soils : earthquakes, traffic, shocks, construction works*, 499 p.

Shukla, S. K., Yin Jian-Hua 2006. *Fundamentals of geosynthetics engineering*, Taylor & Francis group, UK.

Shukla S.K., Gupta S.K., Sivakugan N. 2009. Active earth pressure on retaining wall for c-ϕ soil backfill under seismic loading condition. *J. Geotech. and Geoenv. Engng.*, vol. 135, n°5, pp.690-696.

Zerfa Z., Loret B. 2003. Coupled elastic-plastic analysis of earth structures. *Soil Dynamics and Earthquake Eng.*. 23. 435-454.